

An Exoskeleton Master Hand for Controlling DLR/HIT Hand

Honggen. Fang, Zongwu. Xie, Hong. Liu

Abstract—In order to eliminate the drawbacks of conventional force feedback gloves, a new type of master hand has been developed. By utilizing three "four-bar mechanism joint" in series and wire coupling mechanism, the master finger transmission ratio is kept exact 1:1.4:1 in the whole movement range and it can make active motions in both extension and flexion direction. Additionally, to assure faster data transmission and near zero delay in master-slave operation, a digital signal processing/field programmable gate array (DSP/FPGA-FPGA) structure with 200 μ s cycle time is designed. The operating modes of the master hand can be contact or non-contact, which depends on the motion states of slave hand, free motion or constrained motion. The position control employed in non-contact mode ensures unconstrained motion and the force control adopted in contact mode guarantees natural contact sensation. To evaluate the performances of the master hand, a master-slave control experiment based on Force-Position control method between the master hand and DLR/HIT hand is conducted. The results demonstrate this new type master hand can augment telepresence.

I. INTRODUCTION

HAPTIC interface devices enable the operator interaction with environments that are remote, hazardous, or otherwise inaccessible to direct human contact and provide useful haptic or kinematic information in teleportation tasks and virtual reality applications. They are a key technology area for the effective control of dexterous robots. Recently, many haptic devices for human hand have been developed which can be categorized into two types. One is exoskeleton type. The most representative exoskeleton type are Cybergrasp^[1] and LRP dexterous hand master^[2]. They employ indirect drive method such as using tendon as transmission elements (i.e., the actuators is remote from exoskeleton mechanism), which occupies a larger space and brings complex control problems due to friction and backlash. They must be resided on dorsal side of the phalanx of operator's finger so that the driving force can exert on the segments of operator's finger, which affect the feeling of immersion seriously. The other is endoskeleton type such as the famous Rutgers Master II^[3], which is lightweight, compact and less cumbersome than Cybergrasp and LRP. However, it

restricts the range of operator's finger motion significantly due to the placement of the pistons in the palm and has a lower mechanical bandwidth than Cybergrasp and LRP result from utilizing pneumatic pistons^[4].

McNeely^[5] and Tachi^[6] proposed an encounter-type haptic device. Unlike conventional haptic devices mentioned above, an encounter-type device is not hold by a user all the time. Instead, the device remains at the location of an object and waits for the user to encounter it. Therefore, encounter-type haptic device can provide real free and real touch sensations to the user^[7]. i.e., encounter-type haptic device usually follow the motion of operator's finger without contact when slave

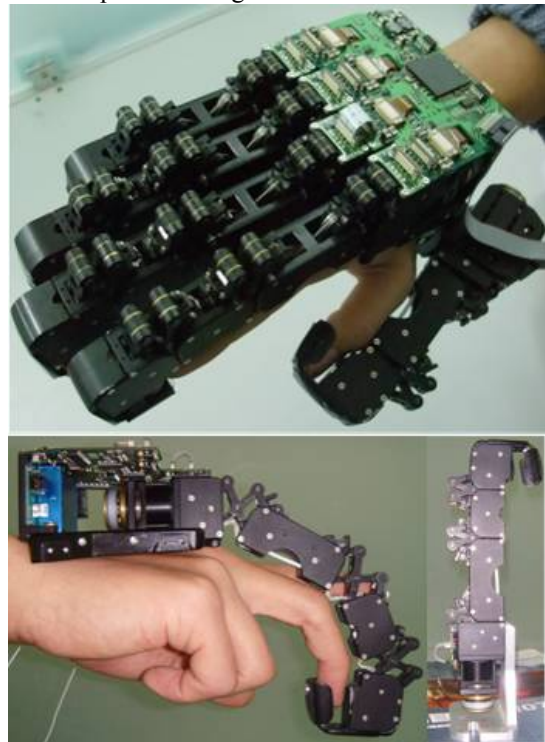


Fig.1 Appearance of the master Hand

end effector is in free space and when in constrained space, it gives a resisting force to operator's finger. Guided by the idea, Nakagawara design a master hand using circuitous joint^[8]. The circuitous joint has disadvantages of complex structure and low mechanical stiffness. As mentioned above, conventional exoskeleton devices for human hand do not satisfy the needs because they should always be grounded to the segments of operator's finger when used. So the master hand (Fig.1) was especially designed to fulfill the requirements.

The success of master-slave operation depends not only on the control algorithm, but also on the hardware controller structure. With the development of the IC technology, some

Manuscript received February 15, 2009. This work was supported by Harbin person with ability of science and technology innovation fund (2008RFQXG053) and the 111 Project (B07018). Honggen. Fang is with the State Key Laboratory of Robotics and System, Harbin Institute of Technology, Harbin, (corresponding author to provide phone: (86-0451-86402330); fax: (86-0451-86418306); e-mail: fangdanwei@163.com).

Zongwu. Xie, is with the State Key Laboratory of Robotics and System. Harbin Institute of Technology, Harbin (e-mail: xiezongwu@hit.edu.cn).

Hong. Liu is with the Institute of Robotics and Mechatronics, German Aerospace Center, Wessling DLR (e-mail: Hong.Liu@dlr.de).

researchers have incorporated control algorithms into FPGA to improve the performance of servo control system. The system developed by Takahashi and Goetz^[9] could run a current control algorithm with a FPGA to increase the bandwidth of the current loop control. FPGA-based motion control has been utilized in other works^[10,11]. In order to realize precise real time control, the ideal minimum cycle time for data transmission is necessary. So a DSP/FPGA structure was proposed to control the master hand and a LVDS serial data bus was designed with 200 μ s cycle time based on the hardware structure.

This paper will be arranged as follows: Section II details the mechanism including “four-bar mechanism joint” of the master finger. Section III describes the multisensory system of the master hand. Section IV presents the DSP/FPGA hardware architecture. Section V analyze and compare the master-slave control method. Section VI presents an experiment conducted to the master hand and DLR/HIT hand. Conclusions are addressed in section VII.

II. THE MECHANISM CONSTRUCTION OF MASTER FINGER

A. Four Bar Mechanism Joint

Two critical facts must be explained in the development of a hand exoskeleton mechanism. One is that the phalanges of the operator’s finger rotate about a point located inside their respective joints. The other is that due to the compact structure of human hand, the limited space decides that placing an exoskeleton mechanism over an operator's finger is more reasonable than beside an operator's finger. To mimic the motion of the operator’s finger, the rotation centers of

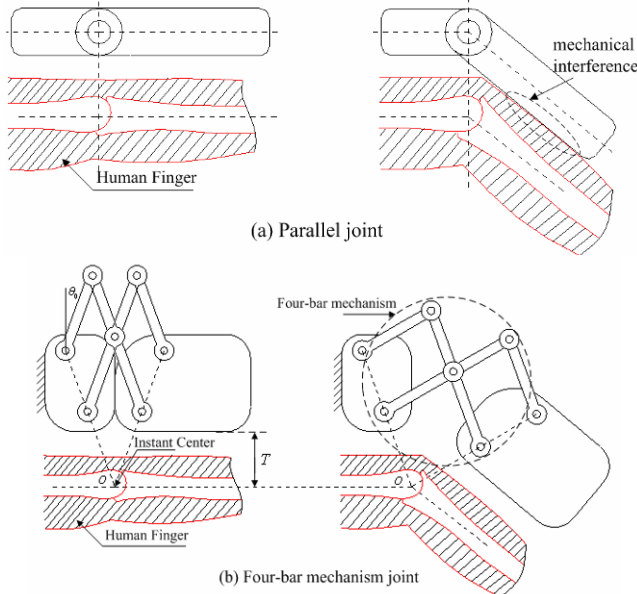


Fig.2 The Scheme of four-bar mechanism

exoskeleton mechanism should coincide with the rotation centers of the operator's fingers to avoid the mechanical interference just as shown in Fig.2 (a) between operator's finger and master finger. The exoskeleton mechanism joint using four-bar mechanism in Fig.2(b) was designed to mimic human finger kinematics. The four-bar mechanism rotates

around an instant center which coincides with that of the operator’s finger. Because of the parallelogram structure of the mechanism, the instant center remains fixed relative to the ground link. The design of each joint mechanism was governed by making the appropriate instant center coincides with the wearer's finger joint center.

B. Master Finger Design

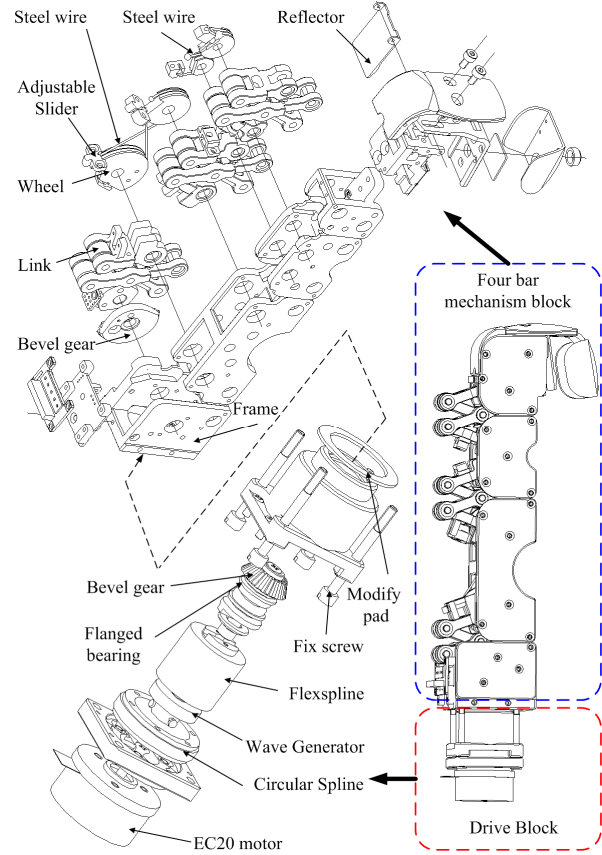


Fig.3 The mechanism design of master finger

The master finger is composed of three same four-bar mechanism joints in series corresponding to finger's joints of operator: metacarpophalangeal joint(MCP), proximal langleinterpha joint(PIP) and distal interphalangeal the master finger. The master hand consists of five modular master fingers assembled on the palm.

TABLE I
SPECIFICATION OF THE MASTER FINGER

Couple transmission ratio		1:1.4:1	
Maximum joint angular velocity	MCP	3.6rad/s	
	PIP	5rad/s	
Maximum joint angular acceleration	DIP	3.6rad/s	
	MCP	69 rad/s ²	
	PIP	97 rad/s ²	
Output force of fingertip		Up to 8N	

joint(DIP). In order to place five modular master fingers on the back of palm, the width of master finger should be as small as possible (width:17mm). As shown in Fig.3, the drive block is made up of brushless motor (Maxon EC20), mini harmonic drive (HDUC-5-100), and bevel gears (reduce ratio 2:1). The middle transmission elements between any two

adjacent four-bar mechanisms employ steel wires and adjustable mechanism, which make it easier to eliminate the mechanical clearance of the master finger than to employ gears and can make active motion in the direction of extension or flexion. Table I summarizes the performances of

III. MULTISENSORY SYSTEM

In order to distinguish contact and non-contact mode in master-slave operation, the master finger utilizes an optical sensor (Sanyo Electric Co.,Ltd.,SPI-314) to detect the distance between tip of operator's finger and that of the master finger as shown in Fig.4. A reflecting plate (thin surperduralumin) and a spring are mounted on an axis. The spring provides a tiny resisting force to the plate, so the operator can hardly sense the force. For sensing the force

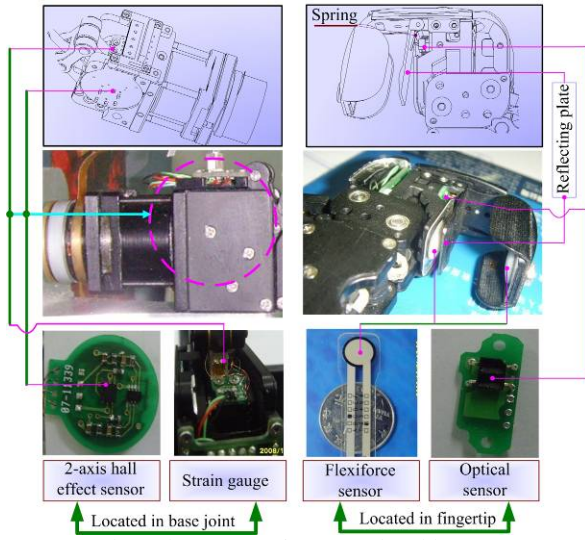


Fig. 4 Finger's Force/Torque and Position Sensor

originating from two directions, two thin force sensors (Tekscan Corporation Flexiforce B201) are located at the upper and lower part of the tip of master finger respectively. In addition, in base joint, there are a strain gauge for calculating the motor torque and a non-contact hall sensor for detecting the angular displacement of the master finger.

IV. DSP/FPGA-FPGA HARDWARE ARCHITECTURE

The DSP/FPGA-FPGA hardware architecture (Fig.5) ensures faster data transmission and real-time control. In the high-level, the DSP (TMS320C6713) is responsible for complex control algorithm, fast computation and communication with PC. The FPGA takes charge of high speed (200 μ s cycle time) LVDS serial data bus communication with low-level. In the low-level, a FPGA (CycloneTM EP1C20) with densities 20060 logic elements and 288Kbits of RAM is chosen to implement BLDC motor control and collection of sensor data for whole master hand. The communication protocol between high-level and low-level based on LVDS is fulfilled by PPSeco (Point to Point High Speed Serial Communication) which is composed of a Point-to-Point, half duplex, and serial communication link.

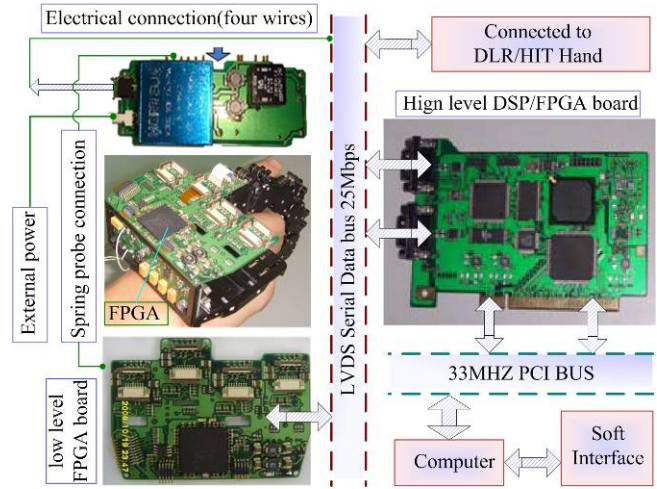


Fig. 5 DSP/FPGA hardware architecture

V. MASTER SLAVE CONTROL METHOD

A. Four channel bilateral control architectures

Important issues for a haptic system are the performance evaluation and controller design for providing a stable high-fidelity system.

1) Stability is of primary concern in feedback control systems. In a teleoperation system, instability can cause an undesirable feeling to the user that distorts the transparent interaction with the environment. It can also be dangerous if the manipulator can output high force or velocities.

2) Once the stability criterion is satisfied, the performance of the system is evaluated. Position/Force tracking and fidelity of the displayed impedance are the two measures employed to determine the performance of the system. Tracking refers to a measure of how well the slave (master) hand can follow the position (force) commanded by the master (slave) hand. Transparency measure is the degree of distortion of the feeling between the operator and remote environment.

In 1993, Lawrence proposed a unified four-channel bilateral control architecture^[12] that communicates the sensed forces and positions from the master to the slave, and vice versa. Fig.6 shows a block diagram of a four-channel teleoperation system with master, slave and communication link models, as well as, operator and environments models. Lawrence asserted that all four channels should be used to obtain transparency.

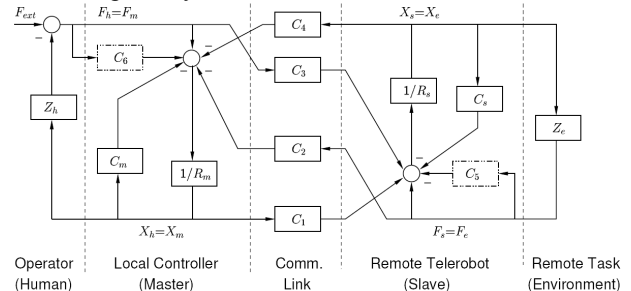


Fig.6 General bilateral control architecture of Lawrence

The master, slave, and communication channel models are

lumped into a linear-time-invariant (LTI) master-slave two-port network (MSN) block. According to Hannaford^[13], it can be represented by a two-port network hybrid matrix:

$$\begin{bmatrix} F_h \\ -X_e \end{bmatrix} = \begin{bmatrix} h_{11} & h_{21} \\ h_{21} & h_{22} \end{bmatrix} \begin{bmatrix} X_h \\ F_e \end{bmatrix} = H \begin{bmatrix} X_h \\ F_e \end{bmatrix} \quad (1)$$

From fig.6 we can get the parameters h_{ij} :

$$h_{11} = \frac{(R_m + C_m)(R_s + C_s) + C_1 C_4}{(1 + C_6)(R_s + C_s) - C_3 C_4} \quad (2)$$

$$h_{12} = \frac{C_2(R_s + C_s) - C_4(1 + C_5)}{(1 + C_6)(R_s + C_s) - C_3 C_4} \quad (3)$$

$$h_{21} = \frac{C_3(R_m + C_m) + C_1(1 + C_6)}{(1 + C_6)(R_s + C_s) - C_3 C_4} \quad (4)$$

$$h_{22} = \frac{(1 + C_5)(1 + C_6) - C_2 C_3}{(1 + C_6)(R_s + C_s) - C_3 C_4} \quad (5)$$

If the hybrid parameters are not functions of Z_h and Z_e , the complete transparency condition can be expressed as:

$$H = \begin{bmatrix} h_{11} & h_{12} \\ h_{21} & h_{22} \end{bmatrix} = \begin{bmatrix} 0 & 1 \\ -1 & 0 \end{bmatrix} \quad (6)$$

Although the four-channel architecture can obtain perfect transparency, they requires measurement of accelerations. This needs complex hardware requirements, so this paper focus on two-channel architectures.

B. two channel bilateral control architectures

Two-channel control architectures are the simplest and most intuitive architectures. In contrast to the four-channel architecture, the two-channel architecture means the relevant constraints are equal to zero. In the following paragraph four typical two-channel bilateral control architectures will be analyzed, in order to select the most appropriate one.

1) Force-Position architecture

In F-P architecture, which is known as flow forward or force feedback, the constraints $C_3 = 0, C_4 = 0$, see Fig.6. Namely, the master position is sent as a command to the slave, while the interaction force at the slave is sent back directly as reaction force to the master, In terms of two-port model and complete transparency condition (6), the control parameters for satisfying perfect transparency must be set as follows:

$$\begin{aligned} C_1 &= R_s + C_s \neq 0; C_2 = 1 + C_6 \neq 0 \\ C_5 &= -1; C_m = -R_m \end{aligned} \quad (7)$$

2) Position-Force architecture

Similarly, in P-F architecture the constraints $C_1 = 0, C_2 = 0$; the idea is to send the interaction force at the master as a reaction force to the slave, and the slave position is passed to the master. The transparency condition (6) is specified as follows:

$$\begin{aligned} C_3 &= 1 + C_5 \neq 0; C_4 = -(R_m + C_m) \neq 0 \\ C_6 &= -1; C_s = -R_s \end{aligned} \quad (8)$$

We can see that the complete transparency can be achieved by using the F-P and P-F architectures, if and only if we select appropriate control parameters C_1, \dots, C_1 and C_s .

3) Position-force architecture

This architecture means the constrains $C_2 = 0, C_3 = 0$. To satisfy the transparency condition, C_5 should be '-1', but it will result in $h_{12} = 0$ and the transparency condition (6) can not be satisfied.

4) Force-Force architecture

Similarly, this architecture means the constraints $C_1 = 0, C_4 = 0$. Likewise, to satisfy the transparency condition, C_m should be '-1', but it will result in $h_{21} = 0$ and the transparency condition (6) can not be satisfied.

From the above-mentioned two architectures, we can see that transparent teleportation is impossible in the P-P and F-F architectures. As a conclusion, in the practical implementation presented in the following section, the F-P architecture will be employed.

C. F-P Architecture Control Method

The present bilateral model is constructed on the basis of the above-mentioned analysis of the F-P two-channel architecture with local force feedback, namely $C_3 = C_4 = 0, C_5$ and C_6 are not equal to zero at the same time. Fig.7 shows the present master-slave control method.

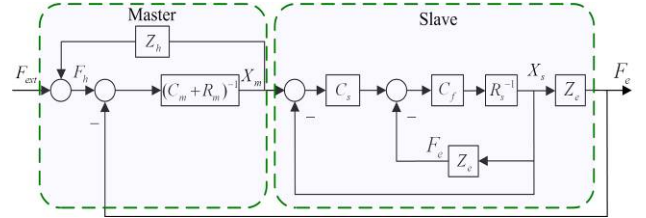
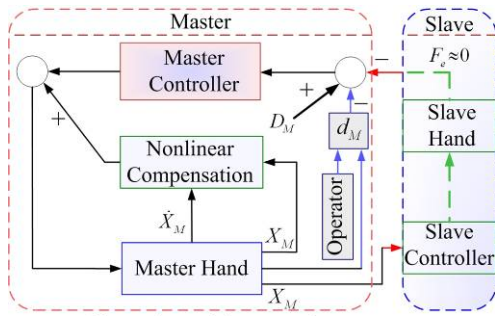


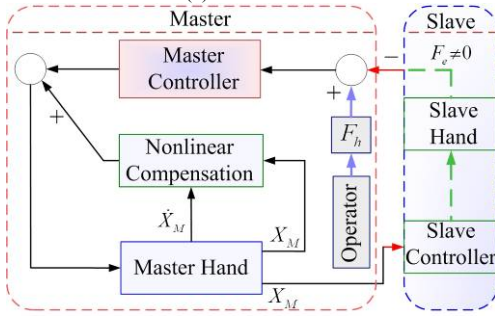
Fig.7 F-P control architecture

The basic function of this system may be described as follows. The human operator exerts a force F_{ext} on the master force sensor so that a motion X_m is generated. The actual motion X_m of the master is measured and transmitted to the slave and executed there by slave motion controller (C_s). The interaction force (F_e) is transmitted back to the master and displayed to the operator. Also, the force is used for modifying the X_m trajectory, resulting in the X_s trajectory.

In order to improve telepresence in free space, the tip optical sensor is used to identify the "non-contact" and "contact" mode clearly, as shown in Fig.8 (a). when the slave is in free space, the master adopts position control to keep the gap (D_M) between the operator's fingertip and its tip at a desired value. When the slave hand touches an object, the master hand is under force control to generate a force that is equal to the force (F_e) applied on the slave (as shown in Fig.8(b)). At the same time, the slave is always position controlled as shown in Fig.7 to follow the same position (X_M) as that of the master. In both of position control and force control, it all employs nonlinear compensation.



Finger tip position control
(a) Non-contact



Finger tip Force control
(b) Contact

D_M : Desire position between master fingertip and operator's;
 X_M : Actual position of master finger;
 F_e : The tip force of slave finger acted by environment;
 d_M : Actual position between master fingertip and operator's
 X_L : Actual position of slave finger
 F_h : The force exerted to master finger by environment

Fig.8 Block diagram of control mode

VI. EXPERIMENTS

A. Master Slave control Experiment

In the experiment as shown in Fig.9, the master hand (configured as master) and a DLR/HIT dexterous hand [14] (configured as slave) are used to implement master-slave

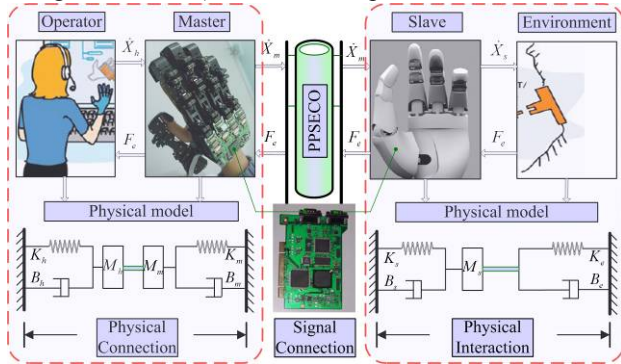


Fig.9 Master-Slave control experiment

operation. They are connected to the ports of DSP/FGPA board. There is a three-axis strain gauge in each dexterous finger which is used to detect the interaction force.

Taking index finger (master, slave) for instance, in the periods (0~4s, 8~11s), the slave doesn't contact any object, so the master-slave operation is working under non-contact mode. The operator's finger extends and flexes back and forth and the master always try to keep desired distance from the tip of operator's finger (Fig.11 and Fig.12). At the same time, the slave almost copies the motion of the master (Fig.12). The

output of the two thin force sensors (master) and that of one dimension of three-axis strain gauge (slave) remain unchanged, which can be seen from Fig.10.

During the periods (4-8s), the slave contacts a soft ball and the master indicates an obvious character: prompt switching from non-contact to contact phases (Fig.10 ~ Fig.12) and maintaining a force that equals to the interaction force. Meanwhile, as shown in Fig.11, the optical reflector holds a fixed position which is the farthest away from the optical sensor thanks to the contact between lower thin force and the abdomen of operator fingertip. The position, velocity (Fig.11) and base torque (Fig.13) keep invariant. This is because the operator's finger should hold a fixed pose to make the slave maintain the contact state. The real torque value is measured by base torque sensor and the theoretical value is calculated by interaction force between operator and the master. It should be noted that in Fig 10, force tracking occurs only when the magnitude of the force applying to the slave exceeds the initial value of the lower thin force sensor.

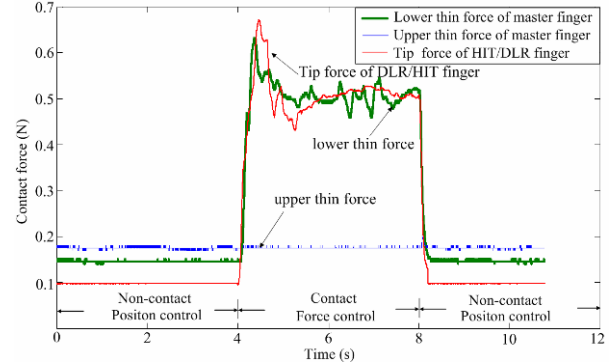


Fig.10 Experimental results of contact force

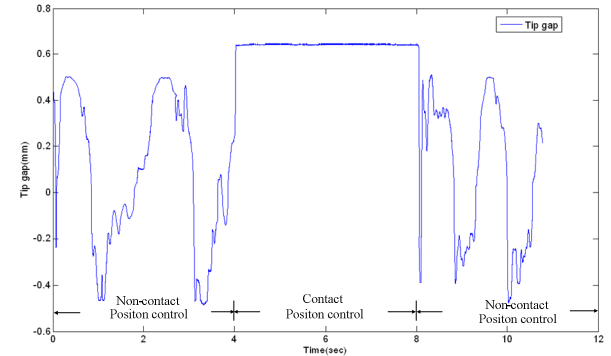


Fig.11 The distance between operator's and master's fingertip

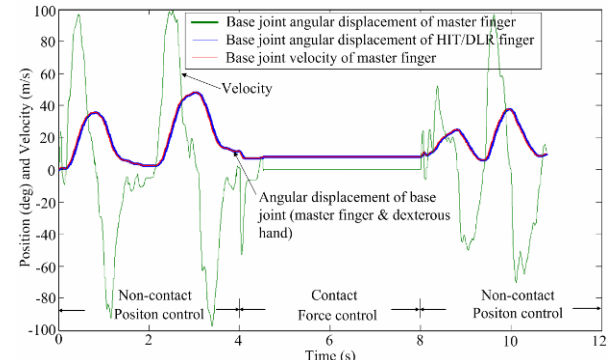


Fig.12 The angular displacement and velocity

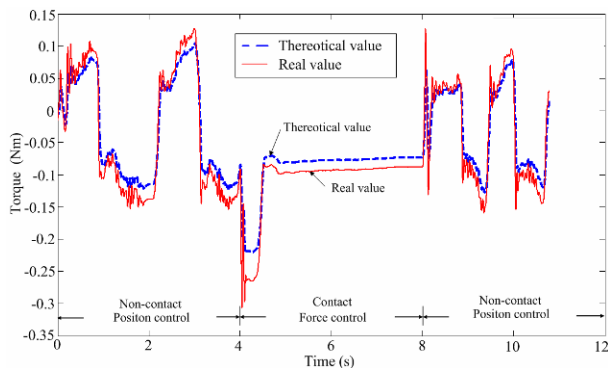


Fig.13 The theoretical torque and real torque

VII. CONCLUSIONS

The traditional force feedback gloves have the following two main disadvantages. (I) They should be grounded to the segments of operator's finger. (II) They can't differentiate contact and non-contact clearly during master-slave operation. These problems can degrade telepresence of master-slave operation.

When the slave hand is in free space, the master hand should provide the operator with unconstrained feeling of free space. But the first shortcoming, friction and other nonlinear factors make it difficult to be achieved.

If the slave hand encounters an object with tiny force (F_s), the master hand should exert the force (F_s) on operator's finger. Using F_c denotes the contact force in free space and assuming that $F_s < F_c$ holds, and then the master controller can't track the force (F_s), so the second deficiency comes out. Even when the condition ($F_s > F_c$) holds, the force (F_s) must be diverted to every segment of the operator's finger owe to the first disadvantage.

To overcome these problems, this paper introduces a new exoskeleton-type master hand. The master hand has key features as followed. (I) It can make extension and flexion motions like the operator's finger without being grounded to it. (II) It has an optical sensor located at its tip which is used for position control to ensure it can track the motion of the operator's finger when the slave is in free space (III) When the slave hand contacts an object, the master hand switches from position control to force control immediately. The second and the third features endow the master hand with the ability of distinguishing contact and non-contact mode clearly. Base on the analysis and comparison of master-slave control methods, the Force-Position control architecture is selected to control the exoskeleton master hand and DLR/HIT dexterous hand.

Finally, a master-slave operation experiment based on DSP/FPGA hardware architecture is conducted. The experimental results prove that the master hand can provide the operator with better feeling of immersion than conventional force feedback gloves.

ACKNOWLEDGMENT

This research is accomplished in DLR/HIT Joint lab. In addition to the authors listed above, Zhang Jizhen also

contributed a lot in the research.

REFERENCES

- [1] Cybergrasp Datasheet. Available: <http://www.immersion.com>.
- [2] M. Bouzit, Design, "implementation and testing of a data glove with force feedback for virtual and real object telemanipulation," Ph.D. Dissertation, Paris, University of Pierre Et Marie Curie, 1996.
- [3] M. Bouzit, G. Burdea, G. Popescu, "The Rutgers Master II new design force-feedback Glove," *IEEE/ASME Trans on Mechatronics*, Vol. 7 Aug. 2002, pp. 256-263.
- [4] C. W. Borst, "Haptic feedback for virtual or mixed reality environments using a combination of passive haptics and active force-feedback," Ph.D. Dissertation, Texas A&M University Computer Science, 2002.
- [5] McNeely, W. A., "Robot Graphics: A New Approach to Force Feedback for Virtual Reality," In *Proceeding of IEEE Virtual Reality Annual International Symposium*, Piscataway, 1993, pp. 336-341.
- [6] Tachi, S., Maeda, T., "A construction method of virtual haptic space," In *Proceeding of the 4th international Conference on Artificial Reality and Telexistence*, Tokyo, 1994, pp. 131-138.
- [7] Y. Yokokohji, N. Muramori, Y. Sato, et al, "Designing an encountered-type haptic display for multiple fingertip contacts based on the observation of human grasping behaviors," *The International Journal of Robotics Reseach.*, vol. 24, Jan. 2005, pp. 1-14.
- [8] Nakagawara, Shuhei, Kajimoto, et al. "An encounter-type multi-fingered master hand using circuitous joints," in *IEEE International Conference on Robotics and Automation*, Barcelona, 2005, pp. 2667-2672.
- [9] Takahashi, Toshio, Goetz, et al, "Implementation of complete AC servo control in a low cost FPGA and subsequent ASSP conversion," in *IEEE Applied Power Electronics Conference and Exposition*, Anaheim, 2004, pp. 565-570.
- [10] Tzou, Y., Kuo, Y., et al, "Design and implementation of an FPGA based motor control IC for permanent magnet AC servo motors," in *23th International Conference on Industrial Electronics, Control and Instrumentation*, New Orleans, 1997, pp. 943-947.
- [11] Dubey, Rahul, Agarwal, et al, "FPGA based PMAC motor control for system-on-chip applications," in *Proceedings of First International Conference on Power Electronics System and Application*, Hong Kong, 2004, pp. 194-200.
- [12] D. A. Lawrence. "Stability and transparency in bilateral teleoperation," *IEEE Transactions on Robotics and Automation*, Vol. 9, 1993, pp. 624-637.
- [13] H. Liu, P. Meusel, N. Seitz, et al, "The modular multisensory DLR-HIT-Hand," *Mechanism and Machine Theory*, vol. 42, July, 2006, pp. 612-625.
- [14] B. Hannaford. "A design framework for teleoperators with kinesthetic feedback," *IEEE Transactions on Robotics and Automation*, Vol. 5, 1989, pp. 426-434.